Fermion Parity of Phases Supporting Multiple Majorana Modes in a Superconducting Nanowire

Alexander Gamov[*]
Siberian Federal University
Krasnoyarsk, Russian Federation
Anton O. Zlotnikov[†]
Kirensky Institute of Physics
Federal Research Center KSC SB RAS
Krasnoyarsk, Russian Federation
Siberian Federal University
Krasnoyarsk, Russian Federation

Abstract. The fermion parity of the ground state is determined in various topological phases of the semiconducting nanowire under external magnetic field with proximity-induced superconductivity and strong spin-orbit interaction. Electron hopping as well as spin-flip hopping due to spin-orbit coupling and superconducting pairings in the second coordination sphere are taken into account. The connection between the fermion parity and the parity of the BDI topological invariant is shown. The formation of topological phases with three and four pairs of Majorana modes has been demonstrated.

Keywords: Fermion parity, superconducting nanowire, Majorana modes, topological invariant, topological phase diagram.

Majorana modes (MMs) that emerge in topological superconductors are of both fundamental and practical interest. This is due to their spatial nonlocality and the potential for implementing non-Abelian statistics through permutations. These characteristics suggest the possibility of utilizing MMs for quantum computing, providing protection against decoherence processes [1–4]. Permutations of non-Abelian anyons result in alterations to the system's ground state wave function. Unlike Abelian anyons (such as fermions and bosons), this change is not solely confined to the introduction of a phase factor.

One of the most renowned systems where the realization of MMs is feasible involves an InSb (or InAs) semiconductor nanowire brought into contact with an s-wave superconductor. For instance, this could be achieved by depositing a 3–5 mm thick layer of aluminum on the nanowire's surface and subjecting it to an external magnetic field [5, 6]. The formation of MMs in such heterostructures was initially predicted in several studies [7–9]. The joint implementation of strong spin-orbit coupling, spin-singlet s-wave superconductivity, and a magnetic field allows the realization of a Kitaev chain regime with effective triplet p-wave superconducting pairings [10]

[*]agamow96@gmail.com   https://orcid.org/0009-0000-3987-4248
[†]zlotn@iph.krasn.ru   https://orcid.org/0000-0003-3195-1397

in the system under consideration. It's essential to note that the experiments have yet to conclusively confirm that the observed signals, such as the conductance peak at zero bias voltage, are precisely associated with MMs and not with trivial Andreev bound states [11, 12].

Typically, in superconducting nanowires, a Majorana bound state is considered, consisting of two MMs localized at opposite ends of the wire. However, the one-dimensional (1D) Hamiltonian used to describe superconducting wires belongs to the BDI symmetry class [13–15], enabling not only non-trivial topology in 1D systems but also the formation of multiple MMs on a single end of a finite-dimensional chain. In this scenario, different MMs on one edge of the chain do not hybridize with each other due to the effective symmetry similar to time-reversal symmetry [16]. Indeed, the realization of a phase with two pairs of MMs (two modes at each edge of the chain) was shown in Refs. [16, 17] when considering extended s-wave superconducting pairings. This implies the presence of pairing interaction between electrons at one site of the chain, as well as between nearest sites. The transition to such a phase can be induced by on-site Hubbard repulsion of electrons [17].

Previously, the formation of topological phases with multiple edge MMs was also shown in chains containing magnetic atoms [18] and under the influence of periodically time-varying external fields [19]. The interest in topological phases with several MMs stems from their realization with arbitrarily small Zeeman splitting of spin subbands (in zero field, they transform into Majorana-Kramers doublets [16]). Additionally, it offers the potential to permute multiple MMs simultaneously in quantum wires of T-, X-, and Y-structures, as was shown for single MMs in [2].

It is natural to assume that in the mentioned systems there also exist non-zero amplitudes of electron hopping, including spin-flip hopping due to spin-orbit coupling, and superconducting pairings between next-to-nearest neighbors in the chain. In this work, considering the processes in the second coordination sphere (CS), we demonstrate the formation of phases with three and four pairs of MMs in the model of a superconductor-semiconductor nanowire with spin-orbit coupling, placed in a magnetic field. Notably, for the classification of regions in the topological phase diagrams, a clear method is employed in addition to the BDI topological invariant [14, 16]. This method is associated with determining the fermion parity (FP) of the system ground state and was previously proposed in Refs. [20–22].

1. Model of a superconducting nanowire in the presence of processes in the second coordination sphere

The Hamiltonian of the model of a superconducting nanowire with open boundary conditions in the tight binding approximation has the form [21]:

$$
\begin{aligned}
H_W =& \sum_{\sigma,n=1}^{N} (-\mu - \eta_\sigma h) C_{n\sigma}^\dagger C_{n\sigma} + \sum_{\sigma,n=1}^{N-1} t(C_{n\sigma}^\dagger C_{n+1\sigma} + C_{n+1\sigma}^\dagger C_{n\sigma}) + \\
&+ \sum_{n=1}^{N-1} \left[(-\alpha)(C_{n\uparrow}^\dagger C_{n+1\downarrow} - C_{n\downarrow}^\dagger C_{n+1\uparrow}) + H.c. \right] + \sum_{n=1}^{N} \left[\Delta_0 C_{n\uparrow}^\dagger C_{n\downarrow}^\dagger + H.c. \right] + \qquad (1) \\
&+ \sum_{n=1}^{N-1} \left[\Delta(C_{n\uparrow}^\dagger C_{n+1\downarrow}^\dagger + C_{n+1\uparrow}^\dagger C_{n\downarrow}^\dagger) + H.c. \right].
\end{aligned}
$$

The first term in (1) characterizes the electron energy measured from the chemical potential μ taking into account the Zeeman splitting h in an external magnetic field. The second term describes hoppings between nearest sites with amplitude t. The third and fourth terms define the Rashba spin-orbit interaction with amplitude α and on-site superconducting pairings with amplitude Δ_0, respectively. The last term is due to superconducting pairings between electrons at nearby sites with the amplitude Δ. It was shown in [16,17] that the formation of phases with two pairs of MMs is possible at $2\Delta > \Delta_0$. To consider this regime in further calculations, it is convenient to set $\Delta_0 = 0$, keeping in mind that the results will be preserved at a qualitative level at $\Delta_0 \neq 0$ and $2\Delta > \Delta_0$. The parameter η_σ determines the sign and takes the following values depending on the projection of the spin momentum σ: $\eta_\sigma = +1$ (at $\sigma = \uparrow$), $\eta_\sigma = -1$ (at $\sigma = \downarrow$).

The Hamiltonian (1) describes only processes in the first CS. Therefore, to take into account long-range hopping, including spin-flip processes, as well as superconducting pairings in the second CS, we add the following terms:

$$
H_2 = \sum_{\sigma, n=1}^{N-2} t_2 (C_{n\sigma}^\dagger C_{n+2\sigma} + C_{n+2\sigma}^\dagger C_{n\sigma}) + \sum_{n=1}^{N-2} \left[(-\alpha_2)(C_{n\uparrow}^\dagger C_{n+2\downarrow} - C_{n\downarrow}^\dagger C_{n+2\uparrow}) + H.c. \right] +
$$
$$
+ \sum_{n=1}^{N-2} \left[\Delta_2 (C_{n\uparrow}^\dagger C_{n+2\downarrow}^\dagger + C_{n+2\uparrow}^\dagger C_{n\downarrow}^\dagger) + H.c. \right]. \tag{2}
$$

The first part of (2) determines the hopping between next nearest sites with amplitude t_2, the second and third terms are responsible for the effective spin-orbit interaction with the parameter α_2 and superconducting pairing with the parameter Δ_2 for the second CS. As a result, the Hamiltonian of the model under consideration is written as:

$$
H = H_W + H_2. \tag{3}
$$

2.   Fermion parity and topological phase diagram

The Hamiltonian of the model in the reciprocal space under periodic boundary conditions takes the form:

$$
H = \sum_{k,\sigma} \xi_{k\sigma} C_{k\sigma}^\dagger C_{k\sigma} + \sum_k \left[\Delta_k C_{k\uparrow}^\dagger C_{-k\downarrow}^\dagger + \Delta_k^* C_{-k\downarrow} C_{k\uparrow} \right] + \sum_k i\alpha_k \left[C_{k\uparrow}^\dagger C_{k\downarrow} - C_{k\downarrow}^\dagger C_{k\uparrow} \right], \tag{4}
$$

where

$$
\xi_{k\sigma} = t_k - \mu - \eta_\sigma h, \quad t_k = 2t\cos(k) + 2t_2\cos(2k), \tag{5}
$$
$$
\alpha_k = 2\alpha\sin(k) + 2\alpha_2\sin(2k), \tag{6}
$$
$$
\Delta_k = 2\Delta\cos(k) + 2\Delta_2\cos(2k). \tag{7}
$$

It was previously shown that the fermion parity (FP) of the ground state of a superconducting system is related to the structure of the Hamiltonian (1) at special points of the first Brillouin zone [20–22]. Here, the special points are considered as those values of the quasimomentum at which either the superconducting order parameter Δ_k or the spin-orbit coupling integral α_k vanishes while having non-zero amplitudes α, Δ, α_2, Δ_2. The identification of such special points is justified by the fact that, as it will be shown later, the Bogoliubov transformations have a different form for these points compared to other BZ points. It is worth noting that for models,

like Bardeen, Cooper, Schrieffer (BCS) model, special points are limited to the nodal points of the superconducting order parameter, where $\Delta_k = 0$. When considering the spin-orbit interaction, the energy spectrum takes a form distinct from BCS theory, although the superconducting gap in the spectrum still closes at the nodal points upon tuning model parameters. However, it can be easily shown in the considered model, that the condition $\alpha_k = 0$ also results in the closing the gap in the elementary excitation spectrum, which could be the cause of a topological transition with a possible change in the ground state FP. In this case, the gap is closed at points where $\alpha_k = 0$ but the superconducting order parameter Δ_k is non-zero. It is important to emphasize that it applies specifically to the closure of the superconducting gap, as in the absence of superconductivity the spectrum becomes gapless on the Fermi contour (lines in BZ).

From (6) and (7) it is obtained that the parameter Δ_k vanishes at the following points:

$$K_\pm = \pi - \arccos\left(\tilde{\Delta}_\pm\right), -K_\pm; \quad \tilde{\Delta}_\pm = \frac{1}{4}\frac{\Delta}{\Delta_2} \pm \frac{1}{4}\sqrt{\left(\frac{\Delta}{\Delta_2}\right)^2 + 8} \in [-1, 1], \tag{8}$$

and the spin-orbit coupling integral α_k vanishes at the points

$$Q = 0, \pi, \quad P = \pi - \arccos\left(\tilde{\alpha}\right), -P; \quad \tilde{\alpha} = \frac{\alpha}{2\alpha_2} \in [-1, 1]. \tag{9}$$

Thus, the Hamiltonian (4) is modified to the following sum of quadratic forms:

$$H = h(0) + h(\pi) + r(P) + r(K_+) + r(K_-) + \sum_{k>0, k \neq Q, P, K_\pm} r(k), \tag{10}$$

where $r(k) = h(k) + h(-k)$ (this definition is also valid for points P, $K_\pm$), and

$$h(Q) = \sum_\sigma \xi_{Q\sigma} C_{Q\sigma}^\dagger C_{Q\sigma} + \Delta_Q C_{Q\uparrow}^\dagger C_{Q\downarrow}^\dagger + \Delta_Q^* C_{Q\downarrow} C_{Q\uparrow}, \tag{11}$$

$$h(P) = \sum_\sigma \xi_{P\sigma} C_{P\sigma}^\dagger C_{P\sigma} + \Delta_P C_{P\uparrow}^\dagger C_{-P\downarrow}^\dagger + \Delta_P^* C_{-P\downarrow} C_{P\uparrow}, \tag{12}$$

$$h(K_\pm) = \sum_\sigma \xi_{K_\pm\sigma} C_{K_\pm\sigma}^\dagger C_{K_\pm\sigma} + i\alpha_{K_\pm}\left[C_{K_\pm\uparrow}^\dagger C_{K_\pm\downarrow} - C_{K_\pm\downarrow}^\dagger C_{K_\pm\uparrow}\right], \tag{13}$$

$$h(k) = \sum_\sigma \xi_{k\sigma} C_{k\sigma}^\dagger C_{k\sigma} + \Delta_k C_{k\uparrow}^\dagger C_{-k\downarrow}^\dagger + \Delta_k^* C_{-k\downarrow} C_{k\uparrow} + i\alpha_k\left[C_{k\uparrow}^\dagger C_{k\downarrow} - C_{k\downarrow}^\dagger C_{k\uparrow}\right]. \tag{14}$$

In [22], it was demonstrated that the eigenfunction of the term $r(k)$ (refer to (14)) can always be expressed as a superposition of states with an even number of fermions, akin to the wave function in BCS theory. Consequently, the structure and FP of the system's ground state are determined by the eigenvectors of the operators $h(Q)$, $r(P)$, and $r(K_\pm)$.

As delineated in [22], the eigenvectors of the term of $h(Q)$ comprise two states: one with a single fermion, denoted as $|F_{Q\sigma}\rangle = C_{Q\sigma}^\dagger|0\rangle$, and two with an even number of fermions, represented as $|\Phi_{Q\pm}\rangle = \left(A_Q^\pm + B_Q^\pm C_{Q\uparrow}^\dagger C_{Q\downarrow}^\dagger\right)|0\rangle$. Of particular interest is the scenario where the state containing one fermion possesses the lowest energy. For $h > 0$ (which is the case always considered here), this reduces to the condition $E_{Q\downarrow}^F < E_{Q,-}^\Phi$. Consequently, the following inequalities emerge:

$$h > \sqrt{\{2t_2 + 2t - \mu\}^2 + |2\Delta_2 + 2\Delta|^2},$$
$$h > \sqrt{\{2t_2 - 2t - \mu\}^2 + |2\Delta_2 - 2\Delta|^2}. \tag{15}$$

The term $r(P)$ has the BCS form, and its eigenvectors also consist of an even number of fermions, leaving FP of the system's ground state wave function unaffected. In contrast, the term $h(K_\pm)$ possesses an eigenvector that can be expressed as a superposition of states with a single fermion: $\left(a_{K_\pm} C^\dagger_{K_\pm \sigma} + b_{K_\pm} C^\dagger_{K_\pm \bar{\sigma}}\right)|0\rangle$ ($\bar{\sigma}$ represents the opposite spin projection to σ). Nevertheless, it's evident that the state $\left(a_{-K_\pm} C^\dagger_{-K_\pm \sigma} + b_{-K_\pm} C^\dagger_{-K_\pm \bar{\sigma}}\right)|0\rangle$, which is appropriate for the term $h(-K_\pm)$, has the same energy. Therefore, even in cases where these states have lower energies than states with an even number of fermions, FP of the ground state wave function remains unchanged because the one-fermion states at points $K_\pm$ and $-K_\pm$ are filled simultaneously. Consequently, the conditions for achieving the ground state of a system with odd FP are dictated by the inequalities (15).

It is important to note that using the quadratic forms highlighted in (10), it is feasible to describe transitions that change the ground state wave function even when FP remains the same. By applying the Bogoliubov transformation, we can determine the excitation energies at the selected k points that may change signs with parameter variations.

$$
\begin{aligned}
E_{1k} &= \sqrt{(t_k - \mu)^2 + |\Delta_k^2|} - h, \quad k = Q, P, -P, \\
E_{2,3k} &= (-\mu) \pm \sqrt{\alpha_k^2 + h^2}, \quad k = K_\pm, -K_\pm.
\end{aligned}
\tag{16}
$$

From the considerations given above, it follows that FP of the ground state for a given set of parameters coincides with the parity of the number of negative energies (16). The energies E_{1Q} at points 0 and π assume negative values under the conditions of (15), respectively. We will now outline the inequalities that lead to the remaining energies becoming negative:

$$
E_{1P,-P} \quad < \quad 0, \quad h > \left\{\left[4t_2(\tilde{\alpha}^2 - 1/2) - 2\tilde{\alpha}t - \mu\right]^2 + \left|4\Delta_2(\tilde{\alpha}^2 - 1/2) - 2\tilde{\alpha}\Delta\right|^2\right\}^{1/2}, \tag{17}
$$

$$
E_{2K_\pm,-K_\pm} \quad < \quad 0, \quad h < \left\{\mu^2 - \mu_c^2\right\}^{1/2}, \quad \mu > \mu_c, \tag{18}
$$

$$
E_{3K_\pm -K_\pm} \quad < \quad 0, \quad h > \left\{\mu^2 - \mu_c^2\right\}^{1/2}, \quad \mu < -\mu_c, \tag{19}
$$

$$
E_{3K_\pm,-K_\pm} \quad < \quad 0, \quad \mu > -\mu_c, \tag{20}
$$

where $\mu_c = 2\sqrt{(1 - \tilde{\Delta}_\pm^2)}(\alpha - 2\alpha_2 \tilde{\Delta}_\pm)$.

Whenever the sign of any of the energies changes, it leads to a modification in the ground state wave function. It is easy to verify that the same conditions correspond to the closure of the gap in the elementary excitations spectrum at special points such as Q, $\pm P$, $K_\pm$, $-K_\pm$, while at other points the spectrum remains gapped until the amplitudes of superconducting pairings are non-zero.

In further calculations, we will assume that all parameters within the same CS are equal to each other. In this context, we will consider $\lambda_1 = \alpha = \Delta = t$ and $\lambda_2 = \alpha_2 = \Delta_2 = t_2$ and explore the case where $\lambda_2 = 1.5\lambda_1$, as it allows for the maximum number of MMs to be realized within the given model. Moreover, to establish the relationship between FP and the parity of the topological invariant, we compute the value of the topological index BDI [14, 16]:

$$
N_{BDI} = \frac{-i}{\pi} \int_{k=0}^{k=\pi} \frac{dz(k)}{z(k)}, \quad z(k) = \frac{\det(Q(k))}{|\det(Q(k))|}, \quad Q(k) = \xi_k \sigma_0 - h\sigma_z - \alpha_k \sigma_y - i\Delta_k \sigma_y, \tag{21}
$$

where σ_0 is the identity matrix, σ_y, σ_z are Pauli matrices.
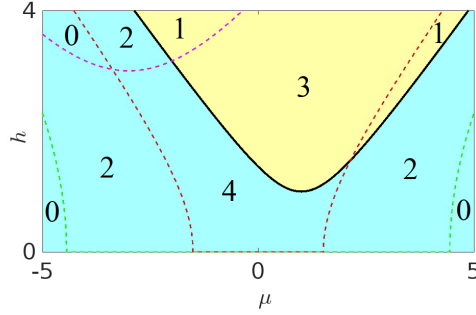
Fig. 1. Topological phase diagram in the variables chemical potential μ — Zeeman splitting h (in units of λ_1) for the amplitude $\lambda_2 = 1.5\lambda_1$. The lines are obtained from the conditions of changing the sign of the energies of one-fermion states at special points of the Brillouin zone. The value of the topological index is marked in each phase. Different colors indicate different fermion parities of the ground state wave function

Fig. 1 illustrates parameter lines $h(\mu)$ where the energy sign changes (16). As indicated in Fig. 1, these lines delineate the regions with distinct values of the topological index. Additionally, these regions are characterized by distinct numbers of negative energies (16). The solid line depicts the dependence (15). Traversing this line results in an energy sign change and a parity shifts in the count of negative energies. The other dependencies, determined from the inequalities (17)–(19), are shown by the dashed lines in Fig. 1. The dashed line obtained from (17) is highlighted in purple, the dependencies (18) and (19) are shown by green and red lines, respectively (see color version). Crossing these lines does not change FP but does modify the form of the ground state wave function. Similarly, when passing through the dashed lines, the topological index changes without affecting its parity. Consequently, the solid line serves as the boundary of the regions in the topological phase diagram with different FP of the wave function of the ground state. The regions highlighted in grey (turquoise in color version) have even FP, and the light (yellow) ones have odd FP.

It can be concluded that the parity of the topological invariant coincides with the parity of the number of one-fermion states that have negative energy in a given region. In this work, we do not specify the precise forms of the ground state wave functions. Their construction is similar to the method described in [22].

It is seen in Fig. 1, that the phases with $N_{BDI} = 3$ and $N_{BDI} = 4$ are formed in the presence of processes in the second CS. It should be noted that the $N_{BDI} = 3$ phase appear even when $\lambda_2 < \lambda_1$ (approximately for $\lambda_2 > 0.5\lambda_1$). And this phase can be realized at low values of Zeeman splitting ($\sim 0.1t$). On the other hand, the $N_{BDI} = 4$ phase is implemented for $\lambda_2 > \lambda_1$.

3.   Majorana modes in phases with $N_{BDI} = 3$ and $N_{BDI} = 4$

To describe features of MMs in the new phases, we consider the Hamiltonian (3) with open boundary conditions and assume that the number of sites is $N = 150$. The transition from the original Fermi operators to Bogoliubov operators is carried out:

$$
\begin{aligned}
a_j &= \sum_{n=1}^{N} u_{jn\uparrow} C_{n\uparrow} + u_{jn\downarrow} C_{n\downarrow} + v_{jn\downarrow} C_{n\downarrow}^{\dagger} + v_{jn\uparrow} C_{n\uparrow}^{\dagger}, \\
a_j^{\dagger} &= \sum_{n=1}^{N} u_{jn\downarrow}^{*} C_{n\downarrow}^{\dagger} + u_{jn\uparrow}^{*} C_{n\uparrow}^{\dagger} + v_{jn\uparrow}^{*} C_{n\uparrow} + v_{jn\downarrow}^{*} C_{n\downarrow}, \ \ j = [-2N, 2N].
\end{aligned}
\tag{22}
$$

The coefficients $u_{jn\sigma}$ and $v_{jn\sigma}$ in this case are components of the eigenfunctions of the Hamiltonian matrix. They can be used to obtain the distribution of quasiparticle operators over the sites of the chain. However in order to spatially separate MMs in the chain, it is convenient to use Majorana operators:

$$
\begin{aligned}
b^{'} &= a_j + a_j^{\dagger} = \sum_{n,\sigma} \omega_{n\sigma} \gamma_{An\sigma} + z_{n\sigma} \gamma_{Bn\sigma}, \\
b^{''} &= i\left(a_j^{\dagger} - a_j\right) = \sum_{n,\sigma} \tilde{\omega}_{n\sigma} \gamma_{An\sigma} + \tilde{z}_{n\sigma} \gamma_{Bn\sigma}, \\
\omega_{n\sigma} &= 2\mathrm{Re}(u_{jn\sigma} + v_{jn\sigma}), \ \ z_{n\sigma} = -2\mathrm{Im}(u_{jn\sigma} - v_{jn\sigma}), \\
\tilde{\omega}_{n\sigma} &= 2\mathrm{Im}(u_{jn\sigma} + v_{jn\sigma}), \ \ \tilde{z}_{n\sigma} = 2\mathrm{Re}(u_{jn\sigma} - v_{jn\sigma}),
\end{aligned}
\tag{23}
$$

where $\gamma_{An\sigma} = C_{n\sigma} + C_{n\sigma}^{\dagger}$, $\gamma_{Bn\sigma} = i(C_{n\sigma}^{\dagger} - C_{n\sigma})$ are Majorana self-conjugate operators.
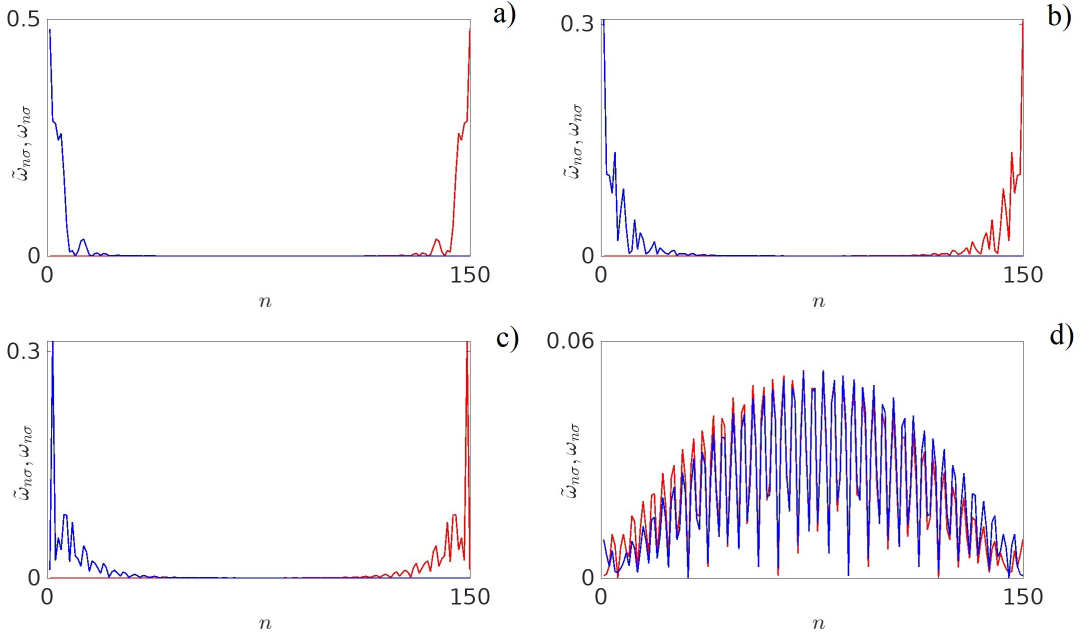

Fig. 2. Distributions of Majorana modes depending on the chain site for the first (a), second (b), third (c) and fourth (d) excitation energies in the phase with $N_{BDI} = 3$. The ratio between amplitudes in the second and first coordination spheres is $\lambda_2/\lambda_1 = 2$

In Fig. 2, the distributions of MMs on the chain sites (coefficients $\omega_{n\sigma}$ and $\tilde{\omega}_{n\sigma}$ in (23)) are presented for the phase with $N_{BDI} = 3$. The dependencies for coefficients $z_{n\sigma}$ and $\tilde{z}_{n\sigma}$ are qualitatively the same. Figures (a–c) reveal that the formation of MMs with edge localization occurs only for the first three excitation energies. These three excitations have near-zero energies (counted from the Fermi level). In the case of the fourth excitation with nonzero energy (d), the probability density of quasiparticles is minimal at the edges of the chain and increases towards to its middle. The probability density of edge states in $N_{BDI} = 3$ phase exhibits an exponential decay with oscillations.

Fig. 3 shows the distributions of MMs for the phase with $N_{BDI} = 4$. As evident from figures (a–d), MMs are formed for all four excitation energies in this phase, resulting in the formation of four pairs of MMs with near-zero energies.
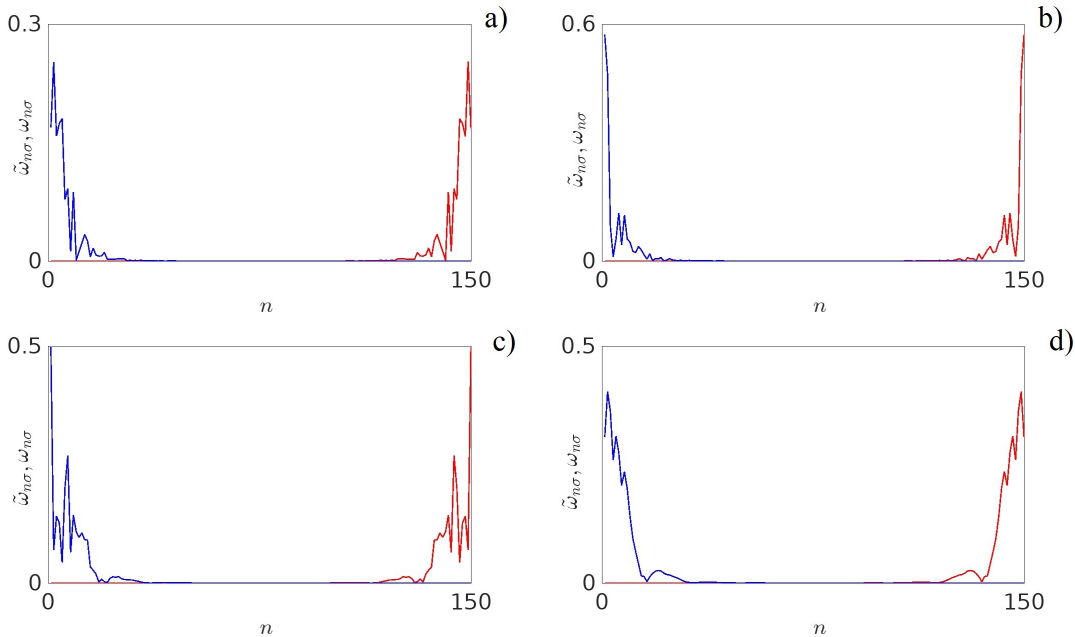
Fig. 3. Site distributions of Majorana modes for the first (a), second (b), third (c) and fourth (d) excitation energies in the phase with $N_{BDI} = 4$ $(\lambda_2/\lambda_1 = 2)$

Conclusion

The model of the superconducting nanowire under external magnetic field is considered with the periodic as well as open boundary conditions taking into account electron hoppings, including spin-flip hoppings due to Rashba spin-orbit coupling, as well as superconducting pairings between nearest and next-nearest neighbors. It is shown for the periodic boundary conditions that different phases on the topological phase diagram can be characterized by the number of occupied one-fermion states that have negative energy at special points of the Brillouin zone. As a result, the region of formation of odd fermion parity of the ground state is determined. It is obtained that the parity of the ground states coincides with the parity of the topological invariant, which in turn indicates the number of Majorana bound states, each of which contains one pair of Majorana modes localized at opposite edges of the chain. We show that taking into account the processes between next-nearest neighbors in a chain with open boundary conditions leads to the formation of phases with three and four pairs of Majorana modes.

References

[1] C.Nayak, S.H.Simon, A.Stern, M.Freedman, S.Das Sarma, Non-Abelian Anyons and Topological Quantum Computation, *Rev. Mod. Phys.*, **80**(2008), 1083–1159.

[2] J.Alicea, Y.Oreg, G.Refael, F. von Oppen, M.P.A.Fishser, Non-Abelian statistics and topological quantum information processing in 1D wire networks, *Nature Physics*, **7**(2011), 412–417. DOI: 10.1038/nphys1915

[3] T.Karzig, F.Pientka, G.Rafael, F.von Oppen, Shortcuts of non-Abelian braidings, *Phys. Rev. B*, **91**(2015), 201102. DOI: 10.1103/PhysRevB.91.201102

[4] F.Harper, A Pushp, R.Roy, Majorana braiding in realistic nanowire Y-junctions and tuning forks, *Phys. Rev. Res.*, **1**(2019), 033207. DOI: 10.1103/PhysRevResearch.1.033207

[5] M.T.Deng, S.Vaitiekenas, E.B.Hansen, J.Danon, M.Leijnse, K.Flensberg, J.Nygard, P.Krogstrup, C.M. Marcus, Majorana bound state in a coupled quantum-dot hybrid-nanowire system, *Science*, **354**(2016), 1557–1562. DOI: 10.1126/science.aaf3961

[6] Microsoft Quantum et al., InAs-Al Hybrid Devices Passing the Topological Gap Protocol, *Phys. Rev. B*, **107**(2023), 245423. DOI 10.1103/physrevb.107.245423

[7] J.D.Sau, R.M.Lutchyn, S.Tewari, S.D.Sarma, Generic New Platform for Topological Quantum Computation Using Semiconductor Heterostructures, *Phys. Rev. Lett.*, **104**(2010), 040502. DOI: 10.1103/PhysRevLett.104.040502

[8] R.M.Lutchyn, J.D.Sau, S.Das Sarma, Majorana Fermions and a Topological Phase Transition in Semiconductor-Superconductor Heterostructures, *Phys. Rev. Lett.*, **105**(2010), 077001. DOI: 10.1103/PhysRevLett.105.077001

[9] Y.Oreg, G.Refael, F. von Oppen, Helical Liquids and Majorana Bound States in Quantum Wires, *Phys. Rev. Lett.*, **105**(2010), 177002. DOI:10.1103/PhysRevLett.105.177002

[10] A.Yu.Kitaev, Unpaired Majorana fermions in quantum wires, *Phys. Usp.*, **44**(2001), 131–136.

[11] C.-X.Liu, J.D.Sau, T.D.Stanescu, S.D.Sarma, Andreev bound states versus Majorana bound states in quantum dot-nanowire-superconductor hybrid structures: Trivial versus topological zero-bias conductance peaks, *Phys. Rev. B*, **96**(2017), 075161.
DOI: 10.1103/PhysRevB.96.075161

[12] S.Das Sarma, In Search of Majorana, *Nat. Phys.*, **19**(2023), 165–170.
DOI: 10.1038/s41567-022-01900-9

[13] S.Ryu, A.P.Schnyder, A.Furusaki, A.W.W.Ludwig, Topological Insulators and Superconductors: Tenfold Way and Dimensional Hierarchy, *New J. Phys.*, **12**(2010), 065010.
DOI: 10.1088/1367-2630/12/6/065010

[14] S.Tewari, J.D.Sau, Topological Invariants for Spin-Orbit Coupled Superconductor Nanowires, *Phys. Rev. Lett.*, **109**(2012), 150408. DOI: 10.1103/PhysRevLett.109.150408

[15] Y. Niu, S.B.Chung, C.-H.Hsu, I.Mandal, S.Raghu, S.Chakravarty, Majorana zero modes in a quantum Ising chain with longer ranged interactions, *Phys. Rev. B*, **85**(2012), 035110.
DOI: 10.1103/PhysRevB.85.035110

[16] C.L.M. Wong, K.T.Law, Majorana Kramers Doublets in dx2-y2-Wave Superconductors with Rashba Spin-Orbit Coupling, *Phys. Rev. B*, **86**(2012), 184516.
DOI: 10.1103/PhysRevB.86.184516

[17] S.V.Aksenov, A.O.Zlotnikov, M.S.Shustin, Strong Coulomb interactions in the problem of Majorana modes in a wire of the non-trivial topological class BDI, *Phys. Rev. B*, **101**(2020), 125431. DOI: 10.1103/PhysRevB.101.125431

[18] A.A.Bespalov, Tuning the Topological state of a helical atom chain via a Josepson phase, *Phys. Rev. B*, **106**(2022), 134503. DOI: 10.1103/PhysRevB.106.134503

[19] H.Wu, S.Wu, L.Zhou, Floquet Topological Superconductors with Many Majorana Edge Modes: Topological Invariants, Entanglement Spectrum and Bulk-Edge Correspondence, *New J. Phys.*, **25**(2023), 083042. DOI: 10.1088/1367-2630/acf0e3

[20] N.Read, D.Green, Paired States of Fermions in Two Dimensions with Breaking of Parity and Time-Reversal Symmetries and the Fractional Quantum Hall Effect, *Phys. Rev. B*, **61**(2000), 10267. DOI: 10.1103/PhysRevB.61.10267

[21] V.V.Val'kov, M.S.Shustin, S.V.Aksenov, A.O.Zlotnikov, A.D.Fedoseev, V.A.Mitskan, M.Yu.Kagan, Topological superconductivity and Majorana states in low-dimensional systems, *Phys. Usp.*, **65**(2022), 2–39. DOI 10.3367/UFNe.2021.03.038950

[22] V.V.Val'kov, V.A.Mitskan, M.S.Shustin, Ground-State Fermion Parity and Caloric Properties of a Superconducting Nanowire, *J. Exp. Theor. Phys.*, **129**(2019), 426–437. DOI: 10.1134/S1063776119080144

Фермионная четность в фазах с множеством майорановских мод в сверхпроводящей нанопроволоке

Александр Гамов
Сибирский федеральный университет
Красноярск, Российская Федерация
Антон О. Злотников
Kirensky Institute of Physics
Федеральный исследовательский центр СО РАН
Красноярск, Российская Федерация
Сибирский федеральный университет
Красноярск, Российская Федерация

Аннотация. Для полупроводниковой нанопроволоки, помещенной во внешнее магнитное поле, с наведенной сверхпроводимостью и сильным спин-орбитальным взаимодействием определена фермионная четность основного состояния в различных топологических фазах при учете перескоков электронов, включая перескоки с переворотом спина за счет спин-орбитальной связи, и сверхпроводящих спариваний во второй координационной сфере. Показана связь фермионной четности и четности BDI топологического инварианта. Продемонстрировано формирование топологических фаз с тремя и четырьмя парами майорановских мод.

Ключевые слова: фермионная четность, сверхпроводящая нанопроволока, майорановские моды, топологический инвариант, топологическая фазовая диаграмма.